International Journal of Heat and Mass Transfer 146 (2020) 118829

Contents lists available at ScienceDirect

International Journal of Heat and Mass Transfer

journal homepage: www.elsevier.com/locate/ijhmt

Film-wise condensation of R-134a, R-1234ze(E) and R-1233zd(E) outside the finned tubes with different fin thickness

Wen-Tao Ji *, Xiao-Dong Lu, Qiu-Nan Yu, Chuang-Yao Zhao, Hu Zhang, Wen-Quan Tao

Key Laboratory of Thermo-Fluid Science and Engineering of MOE, School of Energy and Power Engineering, Xi'an Jiaotong University, Xi'an 710049, China

ARTICLE INFO

Article history:
Received 20 May 2019
Received in revised form 30 September 2019
Accepted 1 October 2019
Available online 15 October 2019

Keywords:
Condensation
Heat transfer
R-1234ze(E)
R-1233zd(E)
Copper tube

ABSTRACT

Film-wise condensation of R-134a, R-1234ze(E) and R-1233zd(E) outside two enhanced tubes was experimentally investigated. The two tubes have the same fin density and similar fin height while the fin thickness is different. In the experiment, the saturation temperature was 36 °C. Heat flux was in the range of 20–90 $kW{\cdot}m^{-2}$. It was found that R-134a was more efficient than other refrigerants and gave the highest heat transfer performance outside the two tubes. R-1233zd(E) was the lowest. Condensing heat transfer coefficient of R-134a was approximately 2 times higher than R-1233zd(E). As heat flux was higher than 20 $kW{\cdot}m^{-2}$, condensing heat transfer coefficient of R-134a and R-1234ze(E) all decreased as the increasing of heat flux. While for R-1233zd(E), up to the heat flux of 90 kW/m^2, the condensing heat transfer coefficient is ever-increasing as the increasing of heat flux. The condensing heat transfer of R-134a was 10–20% higher than R-1234ze(E). The trend of variations for the heat transfer performance of R-134a and R-1234ze(E) was similar. The present work examined the heat transfer characteristics of finned tubes with different fin thickness. It is helpful for the designers to summarize the heat transfer performance of some new HFOs refrigerants having the potential to be used in the water cooled chillers or heat pumps.

1. Introduction

Ozone depletion and global warming are currently two major concerns for the global environment. While, these two critical issues both related with the use of refrigerants. Chlorofluorocarbons (CFCs), hydro-chlorofluorocarbons (HCFCs) and hydro-fluorocarbons (HFCs), although some are prohibited, already have profound effects on the planet. Looking for the sustainable alternatives, environment-friendly, safe, cost-effective, and do not compromise with the performance is the relentless pursuit for the researchers.

In the history, many natural refrigerants were proposed as working media. However, most of them were regarded as unsuitable for various reasons. It is mainly attributable to the flammability, extremely high pressure, toxicity, cost and efficiency. HFCs refrigerants were once regarded as the leading alternatives for CFCs and HCFCs refrigerants. However, higher global warming potential and long atmospheric lifetime are the major reason that many countries would finally give up. Further research shows that, R-134a might be decomposed by sunlight in the troposphere and form poisonous substances. Although not being confirmed yet, high global warming potential will eventually led to the phase out of HFCs by the international treaties.

Hydrofluoroolefins (HFOs) are olefins, composed of hydrogen, fluorine and carbon. HFOs refrigerants have the characteristics of zero Ozone Depletion Potential (ODP) and low Global Warming Potential (GWP). They are considered as the more environmental friendly alternative to HCFCs and HFCs. HFOs that can be used in the refrigeration and air-conditioning systems include 2,3,3,3-tetrafluoropropene (HFO-1234yf), 1,3,3,3-tetrafluoropropene (HFO-1234ze) and 1-chloro-3,3,3-trifluoropropene (HFO-1233zd). R-1234ze(E) is considered as a prospective alternative to the conventional most widely used refrigerant R-134a. R-1234ze(Z) and R-1233zd(E) are expected to be the alternatives of R245fa that might be used in heat pumps, organic Rankine cycles and so on.

The thermophysical properties, cycle performance, boiling and condensing heat transfer of HFOs refrigerants were also investigated intensively recently. For water cooled shell and tube condensers and flooded evaporators, the refrigerant vapor condenses and boils outside the finned tubes. The investigations on the condensation and boiling outside the enhanced tubes mostly include the effect of fin structures, tube material, different refrigerants and experimental conditions. A brief review of such experimental investigations with HFOs is given as below.

* Corresponding author.
E-mail address: wentaoji@xjtu.edu.cn (W.-T. Ji).

https://doi.org/10.1016/j.ijheatmasstransfer.2019.118829
0017-9310/

Park et al. [1] investigated the condensing heat transfer of R-1234yf on plain, low-fin and Turbo-C tubes. The condensation heat transfer coefficients of R-134a and R-1234yf were measured at the saturated vapor temperature of 39 . The wall sub-cooling was from 3 to 8 °C. Experimental results showed that the condensation heat transfer coefficients of R-134a and R-1234yf were almost identical for all the three tubes. The results indicated that in various refrigeration systems the same tube surfaces developed for R-134a could also be used with the HFOs refrigerant R-1234yf. Based upon the measured data, they also proposed a general correlation for predicting the condensation heat transfer of refrigerants outside the plain horizontal tubes.

Rooyen and Thome[2] investigated the nucleate pool boiling heat transfer of refrigerants R-134a, R-236fa and R-1234ze(E) on two enhanced boiling tubes. Pool boiling heat transfer of the single tube in a stagnant pool of liquid refrigerant was measured. The enhanced tubes were Turbo-B5 and Gewa-B5, which were made by Wolverine and Wieland. According to their investigation, R-1234ze(E) had very similar heat transfer performance as R-134a for Turbo-B5 and Gewa-B5 tubes. The tube shape and saturation temperature did not affect the heat transfer significantly. For all the three refrigerants and saturate temperatures, the heat transfer coefficient of Turbo-B5 was nearly constant over the test heat flux. While, there was a decrease in heat transfer coefficient as the increase of heat flux for Gewa-B5. R-236fa had the lowest heat transfer coefficient compared with R-134a and R-1234ze(E) for all the temperatures and heat fluxes.

Nagata et al. [3] investigated the film-wise condensation and pool boiling heat transfer of R-1234ze(E), R-1234ze(Z) and R-1233zd(E) on a horizontal plain tube. The test tube made by copper had the external diameter of 19.12 mm. According to the study, the condensing heat transfer coefficient of R-1234ze(E) was approximately 8% lower than that of R-134a. It could be explained by the 8% lower liquid thermal conductivity and 5% smaller latent heat of R-1234ze(E), relative to R-134a. The condensing heat transfer coefficient of R-1234ze(Z) was approximately 10% higher than R-245fa. It was mostly caused by the 11% lower liquid viscosity and 8% larger latent heat of R-1234ze(Z), relative to those of R-245fa. The condensing heat transfer coefficient of R-1233zd(E) was comparable to that of R-245fa. For the nucleate pool boiling heat transfer, the heat transfer coefficients of R-134a and R-1234ze(E) were obviously higher than those of the other refrigerants. The heat transfer coefficient of R-1234ze(E) was slightly lower than that of R-134a. For R-1234ze(Z) and R-1233zd(E), heat transfer coefficients were a little bit higher and lower than that of R245fa, respectively. These variations of heat transfer coefficient were attributed to the difference of thermo physical properties of the refrigerants.

Chen and Wu [4] recently tested the condensation heat transfer coefficients of R-1233zd(E) outside two horizontal tubes. One tube is plain and the other tube is an enhanced tube, with the internal surface having two-dimensional helical ribs and outside surface having three-dimensional (3D) fins. The saturation temperature was 36.1 °C. It was found that the degree of degradation for the heat transfer performance outside the two tubes was nearly the same for the plain and enhanced tubes. The overall heat transfer coefficient for the enhanced tube is about 8.4 times higher than the plain tube at the same test conditions. Condensing heat transfer coefficient for enhanced surface was approximately 10.8 times greater. This work provides more insights into the physical mechanisms underlying the condensation process on tubes with 3D fins for the HFOs refrigerant.

Up to now, most of studies on the phase change heat transfer for HFOs refrigerants were conducted on the nucleate pool boiling. Measurements on the condensing heat transfer of HFOs refrigerants outside the tubes, especially the enhanced tubes, are still quite limited. The heat transfer performance is a rather important design consideration for the heat exchangers. For a detailed understanding of the heat transfer and provide more reliable data to the industry, it is essential to obtain the condensing heat transfer of different types of enhanced tubes with the above-mentioned low GWP refrigerants. The heat transfer characteristics of finned tubes with different fin thickness are also investigated. Comparing the thermo properties and cost for the existing HFOs refrigerants, R-1234ze(E) and R-1233zd(E) are selected for the present experiments. The heat transfer of HFCs refrigerants R-134a is also studied for comparison. The experimental investigations for different HFOs refrigerants outside plain and enhanced tubes are also compared at the end of this article.

In the past years, some previous researches have been conducted in our laboratory on the condensation of different refrigerants and roughed surfaces, such as [18–20]. However, the effect of 3D fin thickness on the condensing of recently proposed HFOs refrigerants has not been formally investigated in previous papers. For examples, [18] studied the condensation of refrigerants outside the titanium tubes, [19] investigated both the condensing and boiling outside the same surfaces, and [20] examined the influence of condensate on the condensation of R134a outside different enhanced tubes.

2. Experimental apparatus

The schematic diagram of experimental test apparatus is shown in Fig. 1. The condenser has the internal diameter of 147 mm and length of 1.05 m. The condenser is wrapped with rubber plastic for insulation. The thickness of rubber plastic is 60 mm. A thin layer of aluminum foil with thickness of 1 mm is wrapped outside the rubber plastic to prevent the heat radiation heat exchange of experimental apparatus and the environment. Four tubes are fixed in the condenser. Two tubes in the top and two located in the lower position of condenser.

Hot water flows through the tube locates in the lower position of condenser. Liquid refrigerant boils outside the enhanced tube and converts to vapor. Cooling water flows through the test enhanced tubes in the upper position of condenser. Vapor refrigerant condenses outside the test tubes. As the hot water flow through the boiling tubes, the temperature reduces and the cooling water temperature rises when it flows through the condensing test tubes. When the hot and cooling water flows into the water tanks, the temperature was re-adjusted to meet the requirement of experiment. The flow rates of cooling and hot water are all measured with electromagnetic flow meters, which have the accuracy level within 0.1% in the whole measurement range.

High resolution PT100 are used to measure the temperature of refrigerants and water. It has a precision of ±0.05 °C. A digital pressure gauge is used to measure the pressure of refrigerant, which has the precision of 0.01% and test range of 0–2.0 MPa. Keithley digital voltmeter 2700 is used to measure the resistance of PT100. Pressure drop of water inside the tube is measured by a Rosemount differential pressure transmitter. The accuracy of differential pressure transmitter is within 0.1% of full scale (0–37.3 kPa).

The specifications of the test tubes are shown in Table 1, where d_o is the diameter of embryo tube. The photos and cross section of the enhanced tubes is shown in Fig. 2. Tubes C1 and C2 have the identical external fin density and similar fin height, while the fin thickness are different. The fin thickness of C2 is almost twice those of C1. The fins of both tubes are both fabricated with simple three-dimensional structures. The thermal properties of the refrigerants are shown in Table 2.

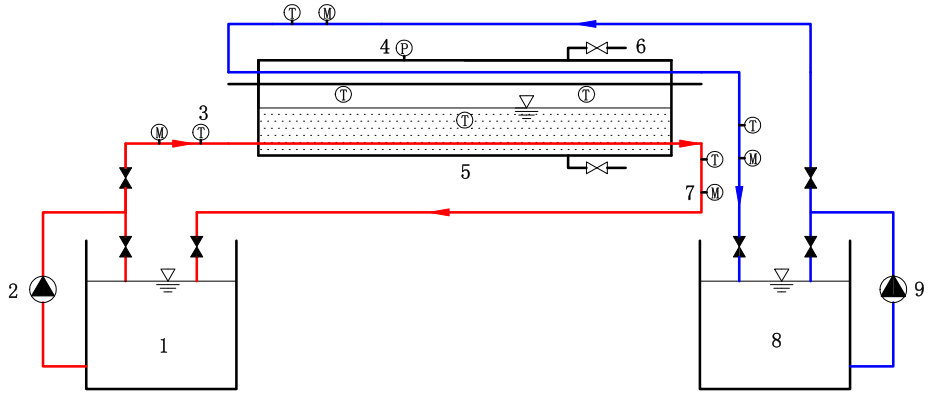

(1) Hot water tank; (2) Hot water pump; (3) Platinum resistance thermometer;

(4) Digital pressure gauge; (5) Condenser; (6) Exhausting valve; (7) Electromagnetic flow meter;

(8) Cold water tank; (9) Cold water pump;

Fig. 1. Schematic diagram of the experimental system.

Table 1
Specifications of test tubes.

Tubes	Outside diameter d_o (mm)	Inside diameter d_i (mm)	Height of inside fin H (mm)	Apex of internal fin θ (°)	Internal starts number	Height of outside fin e (mm)	Ave. External fin thickness δ (mm)	Outside fins per inch
Plain	19.09	16.41	–	–	–	–	–	–
C1	18.99	17.14	0.33	76	50	0.857	0.131	45
C2	19.00	17.12	0.338	59	45	0.790	0.240	45

3. Experimental procedure

After all the test and heating tubes are installed in the condenser, the whole system is charged with nitrogen to check the tightness. The charging pressure is about 1.2 MPa, 1.3 times of the pressure for experimental conditions. Check all the parts of the system to ensure all connections and welds are tight and leak-free. The high pressure should be kept at least 24 h. If no further leakage is detected from the whole system, it can move to the next step.

Then the system is evacuated to the absolute pressure of at least 500 Pa through a vacuum pump. For the experimental system it takes about 1–2 h. In the procedure to fill refrigerant into the system, a small amount of refrigerant is firstly charged into the condenser and then the system is re-evacuated to the absolute pressure of 500 Pa. Repeated this step at least three times until the content of non-condensable gas in the condenser is reduced to the minimum level. Finally, liquid refrigerant is charged into the condenser. The liquid refrigerant should submerge the heating tubes fixed in the condenser. The level of liquid should be at least 50 mm higher than the heating tubes. In the experiment, the amount of the non-condensing gas is checked by two measured saturated temperatures: one is directly measured from the condenser with platinum RTD and the other is got from the measured pressure in the condenser according to the thermo-properties of refrigerant. The difference between these two temperatures is within ±0.1 K. If it does not meet this requirement, the discharging process from the valve fixed in the top of the condenser should be conducted.

In the present work, the experimental data were obtained at the steady state. The steady state in the experiment is featured by: (1) variation of the saturation temperature of refrigerant vapor is in the range of ±0.05 K of directly monitored result, and (2) the fluctuation of water temperature at inlet of condenser were within ±0.1 K. Ten sets of real-time test data should be measured for each individual experimental condition.

4. Data reduction and uncertainty analysis

The heat balance is firstly examined by the heat transfer rate of cooling and heating water.

The power output through cooling water:

$$\phi_c = m_c c_p \left(t_{c,out} - t_{c,in}\right) \tag{1}$$

The heating power from heating water:

$$\phi_e = m_e c_p \left(t_{e,in} - t_{e,out}\right) \tag{2}$$

In the above two equations, $t_{c,in}$ and $t_{c,out}$ are the inlet and outlet temperatures of cooling water (K). $t_{e,in}$ and $t_{e,out}$ are the inlet and outlet temperatures of heating water (K). c_p is the specific heat capacity of water corresponding to the mean temperature of heating and cooling water (J/kg·K). m_c and m_e are the mass flow rates of cooling and heating water (kg/s). The properties of water is obtained from [5].

In the experiment, the maximum difference between the cooling and heating water heat transfer rates are within 5%. The overall heat transfer coefficients of the test tubes are determined by the average of the two heat transfer rates (ϕ). It is calculated using the following equation:

$$k = \frac{\phi}{A_o \cdot \Delta t_m} \tag{3}$$

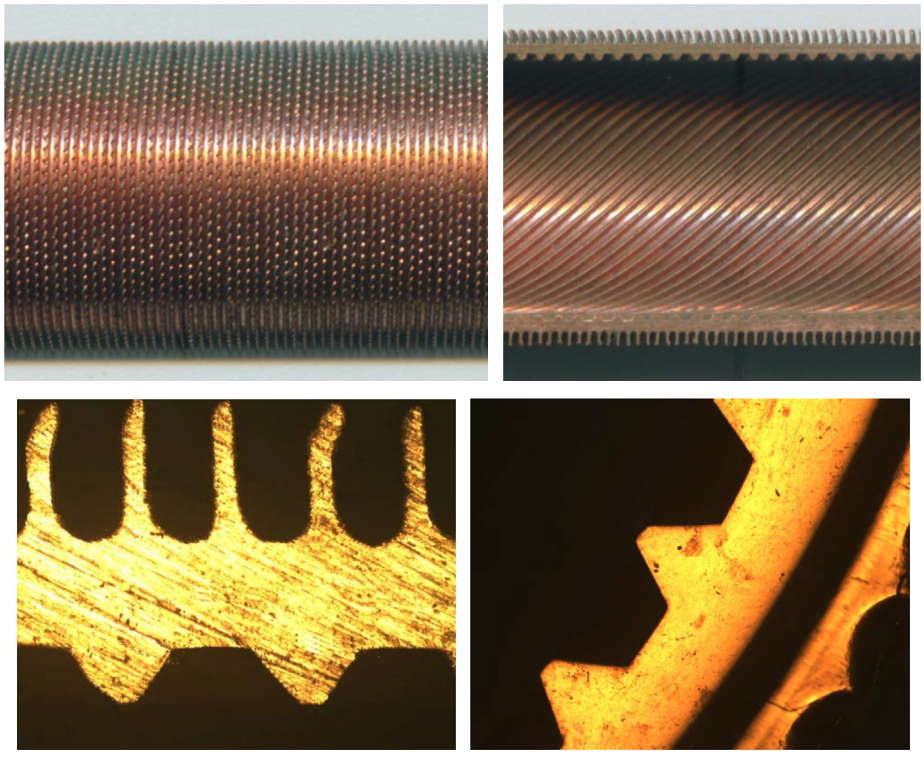

Tube C1

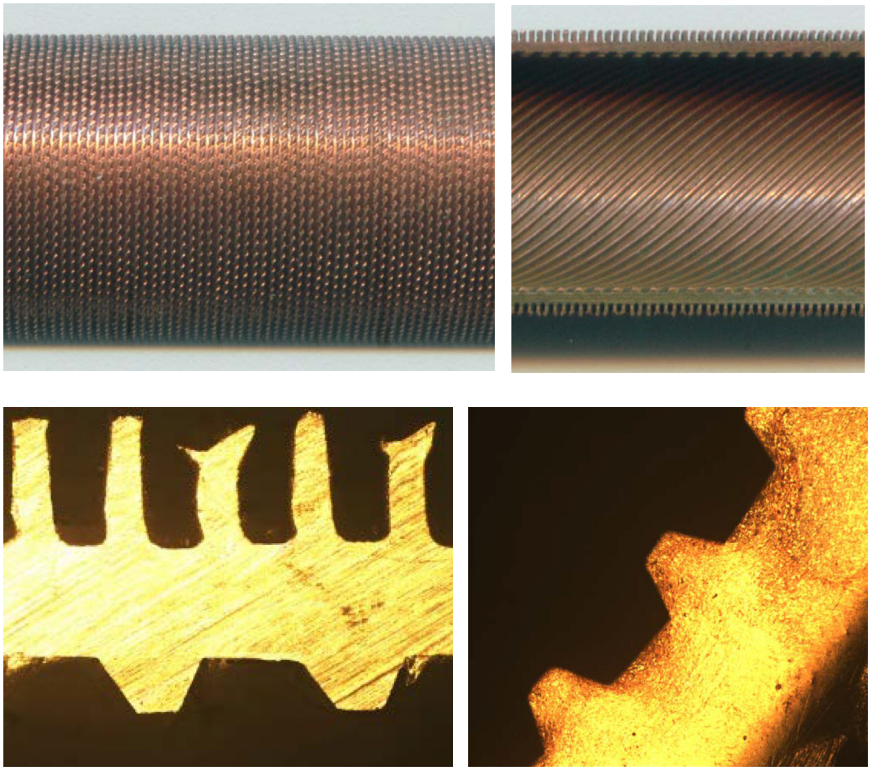

Tube C2

Fig. 2. Photos and cross sections of two enhanced tubes.

where A_o is the outside nominal heat transfer area determined by the outside diameter of the embryo tube, and Δt_m is the log-mean temperature difference, which is defined as follows:

$$\Delta t_m = \frac{|t_{c,in} - t_{c,out}|}{\ln\left(\frac{t_s - t_{c,in}}{t_s - t_{c,out}}\right)} \tag{4}$$

Table 2
Thermophysical properties of test refrigerants.

Refrigerant	T_s (°C)	P (MPa)	Pr	r (kJ/kg)	λ (mW/m·K)	ρ (kg/m^3)	ρ (kg/m^3)	η (μPa·s)	σ (mN/m)
R-134a	36	0.9119	3.28	167.2	76.4	1163.4	44.7	169.9	6.64
R-1234ze(E)	36	0.6866	3.53	158.0	70.7	1125.6	36.3	175.1	7.45
R-1233zd(E)	36	0.1893	3.99	185.3	79.5	1238.2	10.3	247.1	13.13

where t_s is the saturate temperature of refrigerant vapor.

In this study, the condensing heat transfer coefficient is calculated by analyzing different parts of the overall thermal resistance:

$$\frac{1}{k}=\frac{A_o}{A_i}\frac{1}{h_i}+R_w+\frac{1}{h_o} \tag{5}$$

In this equation, $R_w=\frac{d_o}{2\lambda_w}\ln\frac{d_o}{d_i}$, it is the thermal resistance of tube wall. A_i is the internal tube side heat transfer area. If the inner heat transfer tube is plain, then the h_i can be calculated by Gnielinski correlation [6].

$$h_{ip}=\frac{\lambda}{d_i}\frac{(f/8)(Re-1000)Pr}{1+12.7(f/8)^{1/2}\left(Pr^{2/3}-1\right)}\left[1+\left(\frac{d_i}{L}\right)^{2/3}\right]\left(\frac{Pr}{Pr_w}\right)^{0.11} \quad \left(Re=2300-10^6,\quad Pr=0.6-10^5\right) \tag{6}$$

In the correlation above, Filonenko equation ($f=(1.82\lg Re-1.64)^{-2}$) is used to determine the friction factor of internal smooth tube. While, if the internal surface of heat transfer tube is enhanced with internal helical ridges, then the modified Wilson plot method is used to obtain the averaged water side heat transfer coefficient, h_i. The principles of the Wilson plot method are presented in [7]. For integrity, the procedure of this method is briefly introduced as follows.

Heat transfer coefficients for the internal enhanced tubes are typically higher than that predicted by Gnielinski equation [8–10]. The extent of enhancement over the Gnielinski correlation is almost constant if the variation of velocity is not large, typically in the range of 1.5–4. Assuming that the water side heat transfer coefficient can be represented by $c_i h_{ip}$. h_{ip} is the heat transfer coefficient of plain tubes determined by Gnielinski correlation. The nominal heat transfer area for enhanced tube is the same as that for the plain tubes. Other dimensionless characteristic numbers, eg. *Re*, *Nu*, are also the same. The experiment is firstly conducted to determine the constant coefficient c_i. It is the enhancement ratio for the internal helical grooved tube over Gnielinski correlation. In the experiment, the heat flux should be kept constant as h_o is maintained invariant during the test. Then Eq. (5) can be written as:

$$\frac{1}{k}=a\frac{1}{h_{ip}}+b \tag{7}$$

where

$$a=\frac{d_o}{d_i}\frac{1}{c_i} \tag{8}$$

$$b=\frac{1}{h_o}+R_w \tag{9}$$

By changing the tube side water velocity, a group of data is taken and the data can be fitted into a best regression line. The slope a and intercept b in Eq. (7) can be obtained. Then, the enhancement ratio for the internal enhanced tubes, c_i, is determined.

The uncertainty is estimated according to [11–13]. The measurements have a confidence level of 95%. The estimated uncertainties for q are within 5.2%, and that of k is within 5.6%. h_o is not directly measured, and the uncertainty of h_o is estimated using the method proposed by [13,14]. The uncertainties for h_i is 10% according to [15,16]. The estimated uncertainty of h_o for all tubes is within 19.4%.

5. Results and discussion

5.1. Validation of the experimental system

In order to validate the experimental system, the measurements of condensing heat transfer coefficient for plain tube is firstly compared with Nusselt analytical solution [17]. The accuracy has been verified by a variety of refrigerants and plain surfaces [18–20]. The Nusselt analytical solution for film condensation outside the single horizontal tube is shown as below:

$$h_p=0.729\left(\frac{rg\lambda_l^3\rho_l^2}{\mu_l d_o(t_s-t_w)}\right)^{1/4}=0.656\left(\frac{rg\lambda_l^3\rho_l^2}{\mu_l d_o q}\right)^{1/3} \tag{12}$$

Fig. 3 shows the comparison of experimental result and Nusselt analytical solution. The saturation temperature is 40 °C and heat flux is in the range of 10–45 kW/m^2. As shown in Fig. 4, the largest deviation of experimental result and Nusselt analytical solution is 11.8%. The deviation slightly increases as the increase of heat flux. It is mostly caused by the fluctuation of condensate film.

Film Reynolds number of the condensate on one side of tube can be determined by $Re=\frac{4\Gamma}{\mu_l}$. Γ is the total condensate draining rate from the test tube per unit tube length, which is calculated $\Gamma=\frac{\phi}{2Lr}$. In the experiment, the heat flux for smooth tube is within 40 kW/m^2. The condensate film Reynolds number is within 181, in the laminar-flow region. μ_l and r are the dynamic viscosity and latent heat of the condensate at the saturate state, respectively.

5.2. Thermal hydraulic performance of internal helical fins

Fig. 4 shows the Wilson plot for the two enhanced tubes. As shown in Table 1, the internal fin structures are a little bit different. For Tube C1, the internal starts number per circle for C1 is 50 and 45 for C2. In addition, the structure of C1 is a triangle while it is a trapezoid for C2. The slope of Tube C2 is a little bit lower than C1.

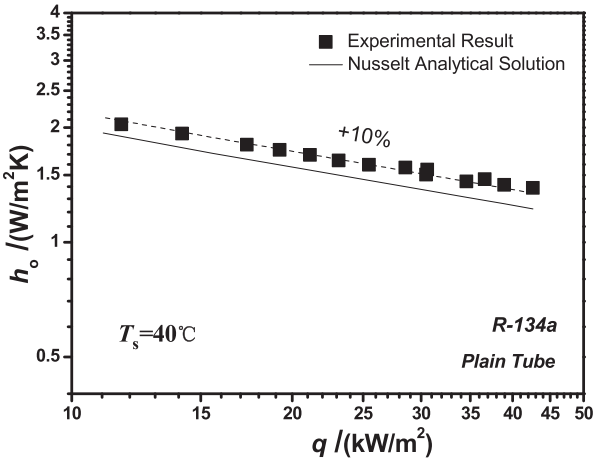

Fig. 3. Comparison of experimental result and Nusselt analytical solution for plain tube.

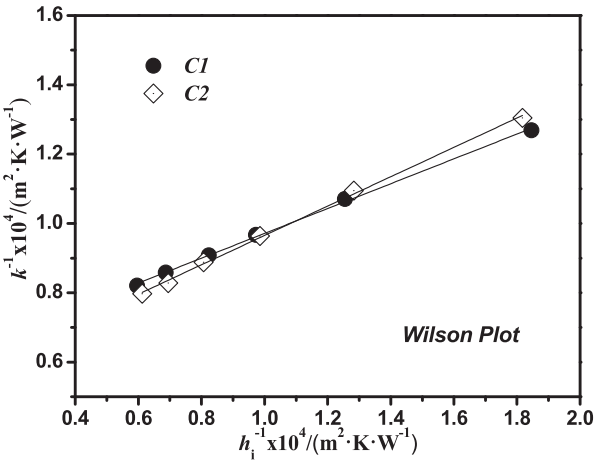

Fig. 4. Wilson plot of two enhanced tubes.

According to fitting straight lines to the experimental data, the enhanced ratios (c_i) for the two enhanced tubes C1 and C2 are 2.96 and 2.62, respectively. The velocity of water is ranging from 1 to 3.5 m/s, at intervals of 0.5 m/s. In the experiment, in order to keep the shell side condensing heat transfer coefficient at the same value, the heat flux in the experiment was maintained at 50 kW/m^2. As the decreasing of water side velocity, the temperature difference is increased to keep the heat flux constant. In the experiment, the variation of heat flux is in the range of ±1500 W/m^2.

The friction factors for the enhanced and plain tubes are shown in Fig. 5. As the heat transfer is intensified, the pressure drop should also increase. The increment ratio of heat transfer is closely related with the pressure drop [8–10]. As shown in the figure, friction factor for plain tube agrees well with the Blasius equation ($f = 0.079Re^{-0.25}$) [21].

The deviation of the experimental data from the correlation is mostly within ±5%. As the number of starts per circle for C1 is 55 and that for C2 is 45, the friction factors for C1 is a little bit higher. For tube C1, the friction factor is 3.63–3.87 times over Blasius equation. It is 3.57–3.75 for C2 tube. At the lower Reynolds number, the difference is a little bit larger. While at higher Reynolds number, the friction factor for the two tubes is almost identical.

The difference for the heat transfer is comparably larger than that for the friction factor. Thermo-hydraulic performance of the internal-finned tubes, Nu/Nu_p vs. f/f_p is shown in Fig. 6. As shown in the figure, for these two enhanced tubes, the increase of friction factors are larger than the increase of heat transfer coefficient. While for many micro-finned tubes, the increase of heat transfer coefficient is very close to the increase of friction factor for water [9,22]. It indicates that the structure of the fins can be further optimized to reduce the pressure drop. If the water side heat transfer enhanced ratio can be increased to the same level as the friction factor, the overall heat transfer performance of the tubes can be further improved.

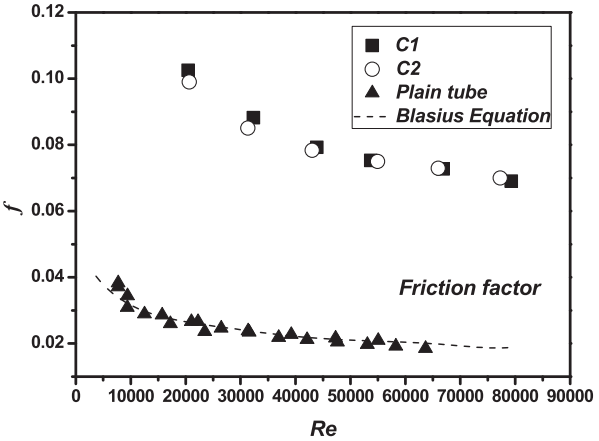

Fig.5. Friction factor versus Reynolds number for plain and enhanced tubes.

5.3. Overall heat transfer coefficient of enhanced tubes

The overall heat transfer coefficients of the three refrigerants over two enhanced tubes are shown in Figs. 7–9. The saturation temperature is 36 °C, and the inlet temperature of water is kept unchanged at 32 °C. The velocity of water inside the tube is from 1 to 3.5 m/s. As the increase of water flow rate, the heat flux in the experiment also increases. The corresponding heat flux in the experiment is in the range of 20–40 kW/m^2. For the three refrigerants, as the increase of water velocity, the overall heat transfer coefficient is also increasing. It indicates that the tube side thermal resistance also plays an important role in the overall heat transfer process.

For the three refrigerants in the present study, R-134a yields the highest overall heat transfer performance. The overall heat transfer coefficient of R-134a outside C1 tube is 7.2–10.6% higher than R-1234ze(E), and 1.7–4.4% higher outside the C2 tube. The difference for R-134a and R-1234ze(E) outside C2 tube is comparably small. The overall heat transfer coefficient for R-1233zd(E) is the lowest, only about one-half of R-134a for the same tube. It is primarily caused by the lower condensing heat transfer coefficient of R-1233zd(E). For the water velocity from 1 to 3.5 m/s, the overall heat transfer coefficient of R-134a and R-1234ze(E) for the two tubes increased about 50% and R-1233zd(E) increased only about 35%. It indicates that the effect of shell side condensing heat transfer for R-1233zd(E) is more pronounced than R-134a and R-1234ze(E).

The overall heat transfer coefficient of C1 is 3.1–9.1% higher than C2 for R-134a. However, R-1234ze(E) and R-1233zd(E) have a different tendency. At the lower velocity, the gaps of the overall heat transfer coefficient for the two tubes are quite small. At higher heat flux, the overall heat transfer coefficient of C2 for R-1234ze(E)

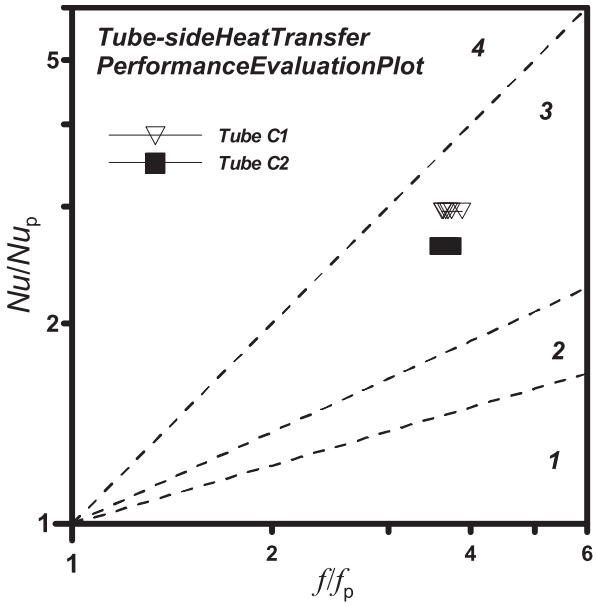

Fig. 6. Tube-side performance evaluation plot for two enhanced tubes.

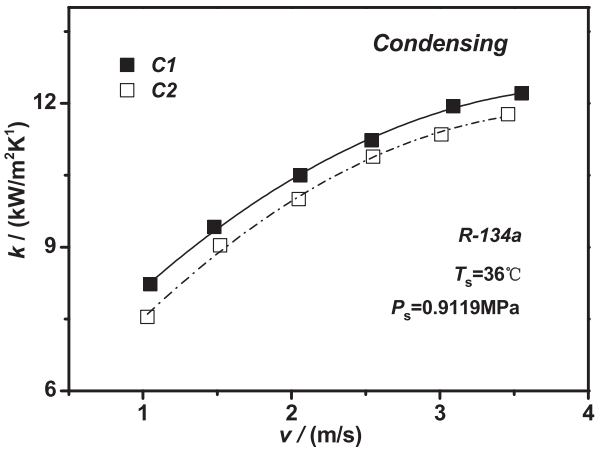

Fig. 7. Overall heat transfer coefficient of R-134a versus water side velocity at saturation temperature of 36 °C on two enhanced tubes.

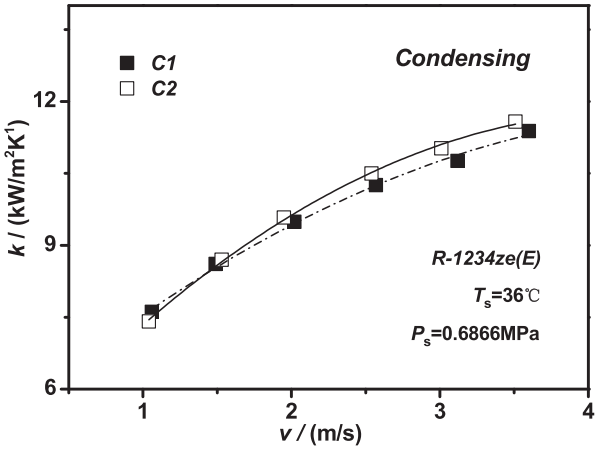

Fig. 8. Overall heat transfer coefficient of R-1234ze(E) versus water side velocity at saturation temperature of 36 °C on two enhanced tubes.

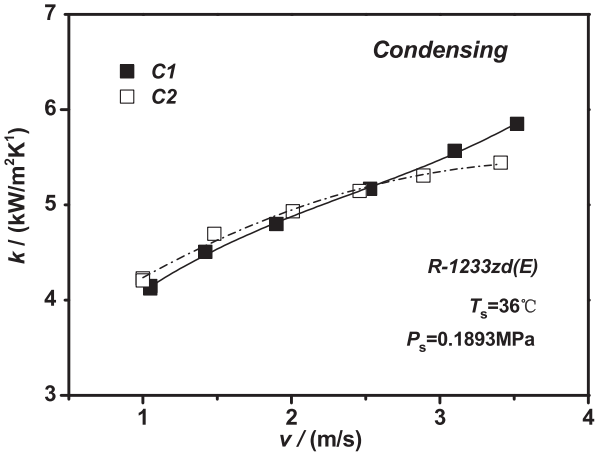

Fig. 9. Overall heat transfer coefficient of R-1233zd(E) versus water side velocity at saturation temperature of 36 °C on two enhanced tubes.

is higher than C1, while it is just contrary to that of R-1233zd(E). The variation is caused by the combined effect of water and shell side heat transfer coefficient. As the enhanced ratio for the tube-side heat transfer coefficient of C1 is 2.96 and C2 is 2.64, and the external condensing heat transfer coefficient of the two tubes is quite similar for R-134a, the overall heat transfer coefficient of C1 is higher at the same velocity for R134a. For R-1234ze(E), the condensing heat transfer coefficients of C2 are higher compared with C1. The effect of shell side condensing heat transfer is larger than that for tube side. Therefore, the overall heat transfer coefficient for tube C2 is a little bit higher than C1. For R-1233zd(E), the overall heat transfer coefficient of C1 at higher water velocity is higher than C2. The reason is that at higher heat flux, the gap in the condensing heat transfer coefficient of C1 and C2 is narrowed, and the heat transfer enhanced ratio for the tube side turbulent flow remains unchanged. Overall heat transfer coefficient represents the overall performance of tubes. It provides the basic heat transfer design parameters for the heat exchangers. The analysis on the shell and tube side heat transfer coefficient can help to optimize the overall heat transfer performance of tubes.

5.4. Condensation heat transfer of enhanced tubes

Condensing heat transfer coefficient of the two enhanced tubes is plotted against heat flux in double logarithmic plot (see Figs. 10–12). The refrigerants include R-134a, R-1234ze(E) and R-1233zd (E). According to Table 2, R-134a and R-1234ze(E) have similar thermal properties. There is a great difference for R-1233zd(E) compared with other two refrigerants. For the two tubes, C1 and C2 have the same external fin density (45fpi), while the fin structure is different. The fin thicknesses of C1 is thinner than C2.

In Figs. 10–12, the comparisons of condensing heat transfer coefficient on the two tubes with different refrigerants are presented. The heat flux is in the range of 20 kW/m^2 to 100 kW/m^2. Saturation temperature in condensing is 36 °C. The main features are described and discussed as follows:

(1) For the three refrigerants, Tube C2, with thicker fin thickness has a relatively higher heat transfer coefficients compared with Tube C1. For R-134a, the condensing heat transfer coefficient of C2 is 0.8–4.1% higher than C1. It was 11.9–13.8% higher than C1 for R-1234ze(E) and 10.3–19.7% higher for R-1233zd(E). The basic trend for the heat transfer performance of two enhanced tubes is generally the same for different refrigerants. It is difficult to quantitatively measure the retention of condensate outside the fins and analyze the stability. As the basic fin structure of two tubes is similar, like the fin density, the difference of heat transfer coefficient is not large. For R134a, it even approaches a negligible value.

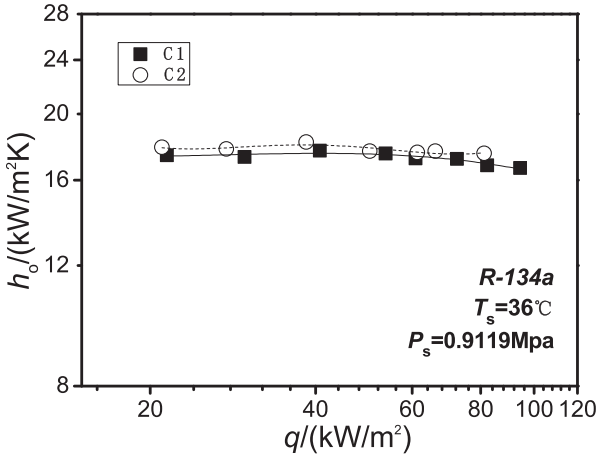

Fig. 10. Condensing heat transfer coefficient of R-134a versus heat flux at saturation temperature of 36 °C on two enhanced tubes.

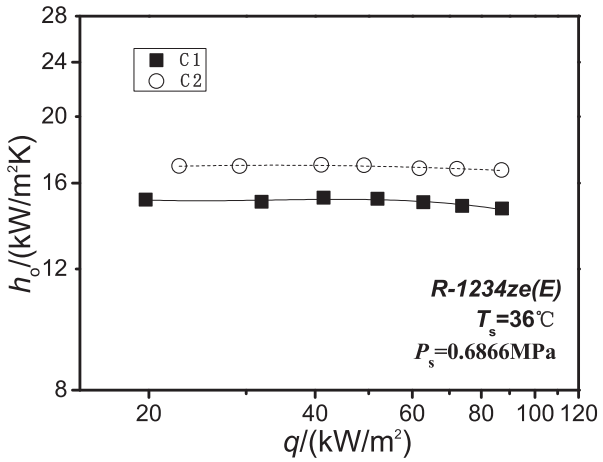

Fig. 11. Condensing heat transfer coefficient of R-1234ze(E) versus heat flux at saturation temperature of 36 °C on two enhanced tubes.

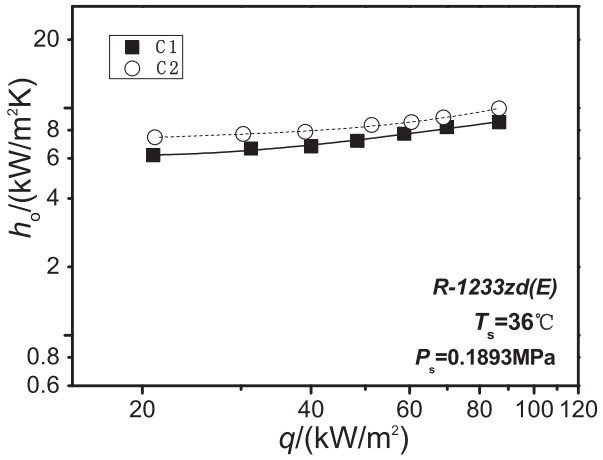

Fig. 12. Condensing heat transfer coefficient of R-1233zd(E) versus heat flux at saturation temperature of 36 °C on two enhanced tubes.

The same decreasing trend is also found for the condensing heat transfer coefficient. From the window in experiment apparatus, it was observed by naked eyes that the condensate retention characteristics were similar, including the condensate drip position and the flow modes. Condensate can be formed on the fin tip, flanks and inter fin tube surface. The other geometries that have effects on the condensing heat transfer also include fin spacing at the fin tips, radii of curvature at the corner of in tip and fin root. Every parameter can cause the liquid to be driven towards different positions. To render the problem to be mathematically available, it is still difficult for the three dimensional structures today. For comparison in the present investigation, it is hard to keep all the parameters to be the same. Only the important parameters were taken into account. As the thermal resistance of shell side condensing heat transfer is normally within 50% of its total thermal resistance for copper tube, if the tube side heat transfer enhancement technique is the same, the difference of corresponding overall heat transfer coefficient should be small when the external fin pitch is same and fin height is similar.

(2) The heat transfer performance of R-134a is a little bit higher than R-1234ze(E), while it is much larger than that of R-1233zd(E). The thermal properties of R-134a and R-1234ze(E) are very similar, including the latent heat, viscosity and surface tension. At the heat flux of 20 to 100 kW/m^2 and saturation temperature of 36 °C, for the tube of C1, the heat transfer coefficient of R-134a was 14.4–15.9% higher than R-1234ze(E). The difference was not obvious for C2. It was only 3.8–6.9% higher for R-134a compared with R-1234ze(E). It indicates that for the same fin structures, the heat transfer performance is different for different refrigerants.

(3) For R-134a and R-1234ze(E), the heat transfer coefficient is decreasing as the increasing of heat flux. While for R-1233zd(E), the heat transfer coefficient is increasing as the increase of heat flux. At the heat flux from 20 to 90 kW/m^2, the heat transfer coefficient increased by about 30%. This kind of reversal phenomenon might be associated with the lower heat transfer performance of this refrigerant outside the two tubes. As the increase of heat flux, the rate of condensation gradually increases on the enhanced surfaces. The two enhanced tubes can have higher heat transfer performance while it is lower for R-1233zd(E). It indicates that the enhanced structures are capable of discharging the condensate and maintains a higher value of heat transfer coefficient. Limited by experiment conditions, the heat flux in the experiment is in the range of 20–90 kW/m^2. The condensing heat transfer coefficient might decrease when the heat flux reaches a critical value. The same increase of heat transfer coefficient as the increase of heat flux or sub cooling is also observed in the literature for different types of enhanced tubes [23–26], especially the tubes or refrigerants that had lower heat transfer coefficient. The reason for this phenomenon is still not clear and further study is needed.

As shown in the figure, the optimum fin structure for the heat transfer performance is dependent upon the refrigerant. Compared with the investigation in the literature, condensing and pool boiling heat transfer for R-1233zd(E) are all less than R-134a and R-1234ze(E) [3]. The heat transfer coefficient of R-1234ze(E) is a little bit lower than R-134a. It is consistent for the present investigation and that from literature. For the present study, the enhanced tube with thicker fin thickness, the enhanced ratio is higher than the tube with thinner fins.

According to the analytical model of Webb et al. [27], for the tubes with same fin density and fin height, thicker fins should have lower heat transfer coefficient. The narrow gaps for Tube C2 should have more retention in terms of flooded area compared with Tube C1. However, it is found that the condensing heat transfer relates to more than just the fin thickness, which is also in relevant with the fin structure. Fin structure also has an obvious effect on the condensing heat transfer. According to the present investigation, for R134a, the two tubes have very similar heat transfer coefficient; for the other two refrigerants, tube C2 has higher heat transfer coefficient at the same heat flux. The tubes in the present investigation are both modified more or less into the three dimensional structures. Modifications on the basic structure are a little bit different. The top of Tube C2 have a deeper indentation, and the fins of Tube C2 have smaller bends in the top, which also have stronger effect on the condensing heat transfer characteristics.

It is difficult to analyze the fin efficiency of integral fins with some three-dimensional modifications in condensation. The fin efficiency for the three dimensional enhanced tube is different from the two dimensional low fin tubes. For the two dimensional tubes, the fins with lower thickness has higher heat transfer coefficient. In order to compare the difference, Fig. 13 shows the experimental condensing heat transfer coefficient of Tube C1 and that from predication result of regular low-fins (take the average value of fin pitch, height and thickness for the regular low-fin).

Beatty-Katz [28] and Webb [27]'s models which ignore the three dimensional effect resulted in much lower prediction performance than the experimental result at the higher heat flux. At the lower heat flux, the prediction result of heat transfer coefficient for low-fin tube is approaching Tube C1. It indicated that the three dimensional effect cannot be ignored for the fins.

The effect of *Pr* number and other parameter is also analyzed (Figs. 14 and 15). In the figures, *Nu* is the Nusselt number of film condensation. Characteristic length is the external diameter d_o. Prandtl numbers for R134a, R1234ze(E) and R1233zd(E) at 36 °C are 3.28, 3.48, and 3.77. Prandtl number is a dimensionless number representing by the ratio of momentum diffusivity to thermal diffusivity. The steady film wise condensation is largely dependent on the film thickness of condensate, and the larger Pr, the lower of thermal diffusivity. That's one of the reason the heat transfer coefficient of R1233zd(E) is lower than the other two refrigerants. Another important factor that has effect on the condensing heat transfer coefficient is surface tension. The surface tension for R134a, R1234ze(E) and R1233zd(E) at 36 °C are 6.64, 7.58, and 13.13, respectively. Higher surface tension tends to reduce the condensate film thickness at the upper part of fins. However, it also tends to retain the condensate between the fins, especially the fins with higher fin density. Retention of condensate outside the fins would decrease the condensing heat transfer to a certain extent. For the two enhanced tubes, refrigerants with larger surface tension have a comparably lower condensing heat transfer coefficient.

The typical HFOs refrigerants having the potentials to be used in the water cooled chillers include R1234yf, R-1234ze(E), R-1234ze (E) and R-1233zd(E). These refrigerants are considered as the alternatives to R-134a for the chillers. A comparative study on the condensing heat transfer of these R1234yf, R-1234ze(E), R-1234ze(E) and R-1233zd(E) refrigerants outside different tubes is also performed in this study. The comparison includes the experimental investigation on the condensation heat transfer of these HFOs refrigerants on the plain and enhanced tubes [1,3,4,18,29]. For ease of comparison, the experimental data of present study for R-134a are also provided.

As shown in Fig. 16 for the plain tubes, R1234yf has the highest heat transfer performance at the higher heat flux. Because the latent heat of vaporization for R-1234ze(Z) is higher than the other refrigerants [30], the heat transfer performance of R-1234ze(Z) was higher than R-134a. Experimental data of R-1234ze(E) for plain tubes in [3,18,29] are in good agreement with each other at different heat flux. The heat transfer coefficient of R-134a for the plain tubes is approximately 5–10% higher than R-1234ze(E). The tube material for Ji et al. [18] is titanium. The deviation of experimental

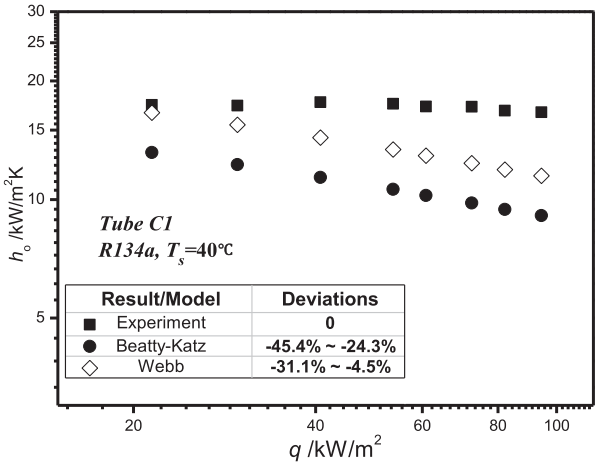

Fig. 13. Comparison of experimental condensing heat transfer coefficient and Beatty-Katz and Webb's models.

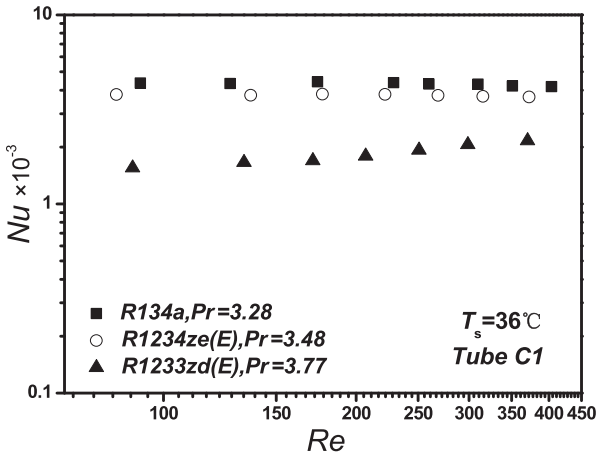

Fig. 14. Condensing heat transfer *Nu* versus condensate *Re* for Tube C1.

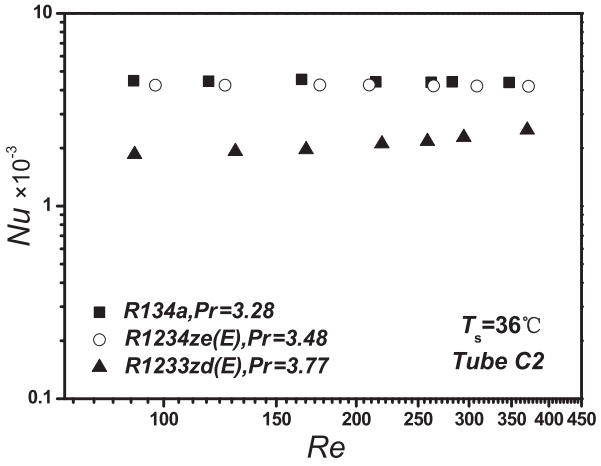

Fig. 15. Condensing heat transfer *Nu* versus condensate *Re* for Tube C2.

data for R-1234ze(E) from other copper plain tubes are also within 6%. It proved that the condensing heat transfer coefficient is independent of metal tube material for the plain surfaces. Large inconsistency exists for the condensing heat transfer coefficient of R-1233zd(E). In the study of Ko et al. [29], the heat transfer coefficient is the lowest, while it is pretty higher for the data in [3]. The experimental data of Nataga et al. [3] is approximately 15–26% higher than that in Ko et al. [29]. This indicates the data are still insufficient and more studies are still required for R-1233zd(E).

Fig. 17 compares the condensing heat transfer performance outside the enhanced tubes. According to the literature survey, only four enhanced tubes are available for the HFOs refrigerants in condensing. It includes two low-fin and two three-dimensional enhanced tubes. The low-fin tube in Ji et al. [18] is also made by titanium. It should have lower heat transfer performance than the copper tubes, because the fin efficiency is lower for the tubes with lower thermal conductivity. As shown in the figures, the 3D enhanced tubes for R-1234ze(E) and R1234yf have similar heat transfer coefficient as R-134a. The gap for the experimental data of R-1233zd(E) outside the enhanced surfaces is also relatively large, similar with the plain tubes. The heat transfer coefficient of 3D enhanced tubes in Chen and Wu [4] is the highest. While the heat transfer coefficient outside another 3D surface of present data is significantly lower than the tubes in [4]. It might be caused by the difference in surface structures. For the flow condensation and boiling, the heat transfer coefficients of R-1234ze(E) and R-134a are also very close [31].

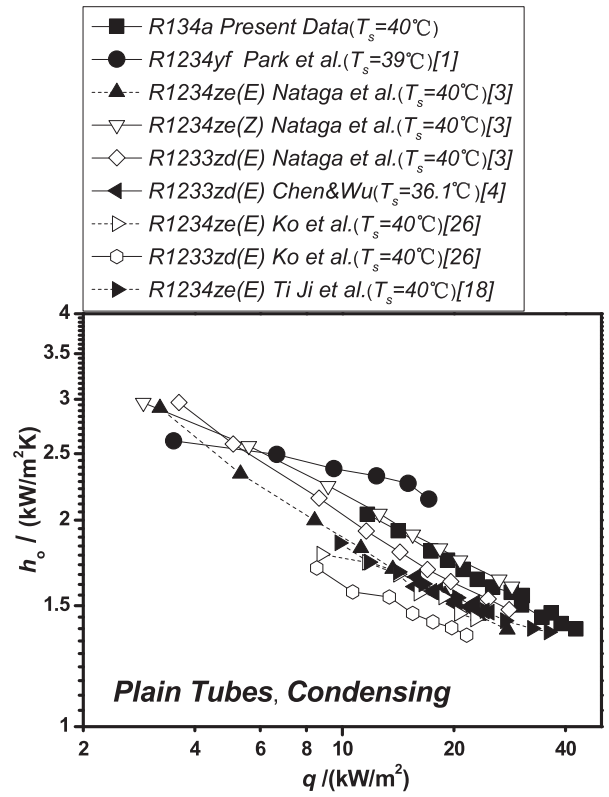

Fig. 16. Condensing heat transfer coefficient of HFOs versus heat flux outside plain tubes in literature.

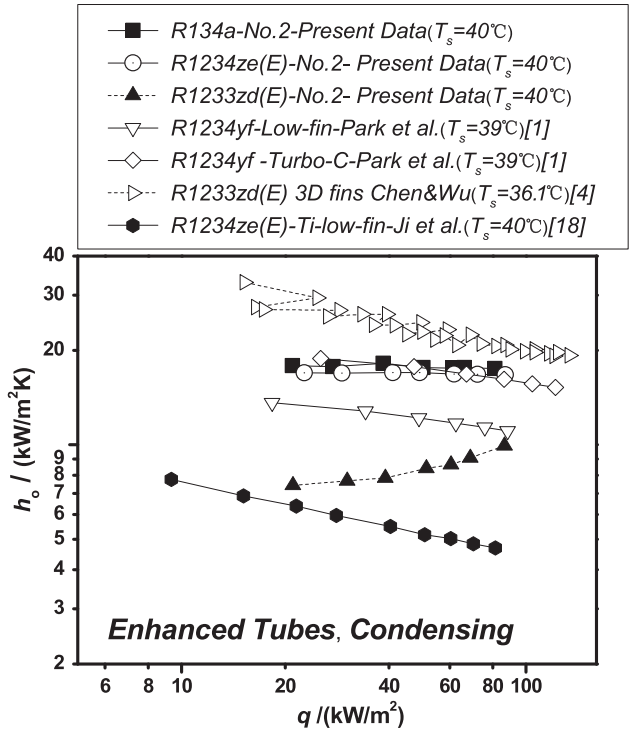

Fig. 17. Condensing heat transfer coefficient of HFOs versus heat flux outside enhanced tubes in literature.

These comparisons show the following features for the condensation of HFOs refrigerants: firstly, for the plain tube, the basic characteristics of different refrigerants can be exhibited, such as the five refrigerants in comparison. Except that for R1234yf, the slopes for different types of refrigerants are similar, a constant −1/3 as suggested by Nusselt analytical solution [17]. Secondly, the mechanism in condensation for the enhanced tubes is rather complex. The slope of the heat transfer coefficient is different for different fin structures. The variation of heat transfer coefficient is also difficult to predict. Thirdly, the condensing heat transfer performance is dominated by the combined effect of refrigerants and fin structures. For condensing, latent heat, viscosity and surface tension are the important factors, which directly affect the condensing heat transfer. The differences in properties can be exhibited by the heat transfer. For R-1233zd(E) in the present study, the vapor density is the lowest and viscosity is the highest compared with the other two refrigerants. It leads to the lower heat transfer coefficient of R-1233zd(E) in the present study. Fourthly, for the effect of fin structure, the three dimensional structure with thicker fins is beneficial to the condensing heat transfer compared with thinner fins in the present study. For different refrigerant, the effect was also different, e.g. R-134a in the present study. Using the thinner fins with the same fin density can have the same heat transfer performance as that with thicker fins. Fifthly, the HFOs refrigerants can have the similar heat transfer performance as HFCs or HCFCs refrigerants. The fin structure or spacing of present two enhanced tubes might not be an optimum structure. Optimization on the fin structure for HFOs refrigerants can further improve the heat transfer. For the energy saving and global environmental protection considerations, these refrigerants in the refrigeration or heat pump can have the equivalent performance as that with HFCs and HCFCs refrigerants, e.g. R-134a, R22 and R123.

6. Conclusions

Condensing heat transfer of R-134a, R-1234ze(E) and R-1233zd (E) were experimentally investigated on the two three-dimensional enhanced tubes. In experiment, saturation temperature was 36 °C. Heat flux was ranging from 20 to 90 kW/m^2. Based on the experimental result the major findings are as follows:

(1) The condensing heat transfer coefficient of R-134a outside the two typical enhanced tubes is higher than R-1234ze(E). R-1233zd(E) is the lowest. For different refrigerants, the magnitude of difference is dependent upon the tubes.
(2) For the present two tubes, the condensing heat transfer coefficient of finned tube with thinner fin thickness is lower than that with thicker fins. For R-134a and R-1233zd(E) the difference is smaller than that for R-1234ze(E).
(3) For the two enhanced tubes, the heat transfer coefficient is increasing as the increase of heat flux for R-1233zd(E). For R-134a and R-1234ze(E), the heat transfer coefficient is decreasing as the increasing of heat flux.
(4) As the basic fin structures of tubes are similar, like the fin density and height, the difference of heat transfer coefficient is not large for different refrigerants.

Declaration of Competing Interest

The authors declare that they have no known competing financial interests or personal relationships that could have appeared to influence the work reported in this paper.

Acknowledgment

This work was supported by the National Natural Science Foundation of China (51776160) and the 111 Project (B16038).

References

[1] K.-J. Park, D.G. Kang, D. Jung, Condensation heat transfer coefficients of R1234yf on plain, low fin, and turbo-C tubes, Int. J. Refrig. 34 (2011) 317–321.
[2] E.V. Rooyen, R.J. Thome, Pool boiling data and prediction method for enhanced boiling tubes with R-134a, R-236fa and R-1234ze(E), Int. J. Refrig. 36 (2013) 447–455.
[3] R. Nagata, C. Kondou, S. Koyama, Comparative assessment of condensation and pool boiling heat transfer on horizontal plain single tubes for R1234ze (E), R1234ze (Z), and R1233zd (E), Int. J. Refrig. 63 (2016) 157–170.
[4] T. Chen, D. Wu, Enhancement in heat transfer during condensation of an HFO refrigerant on a horizontal tube with 3D fins, Int. J. Therm. Sci. 124 (2018) 318–326.
[5] N.R.P.D. 23, REFPROP, NIST, Gaithersburg, MD, 1998.
[6] V. Gnielinski, New equations for heat and mass transfer in turbulent pipe and channel flows, Int. Chem. Eng. 16 (1976) 359–368.
[7] J.W. Rose, Heat-transfer coefficients, Wilson plots and accuracy of thermal measurements, Exp. Therm. Fluid Sci. 28 (2004) 77–86.
[8] W.T. Ji, D.C. Zhang, Y.L. He, W.Q. Tao, Prediction of fully developed turbulent heat transfer of internal helically ribbed tubes-an extension of Gnielinski equation, Int. J. Heat Mass Transfer 55 (2011) 1375–1384.
[9] W.T. Ji, A.M. Jacobi, Y.L. He, W.Q. Tao, Summary and evaluation on single-phase heat transfer enhancement techniques of liquid laminar and turbulent pipe flow, Int. J. Heat Mass Transfer 88 (2015) 735–754.
[10] W.-T. Ji, A.M. Jacobi, Y.-L. He, W.-Q. Tao, Summary and evaluation on the heat transfer enhancement techniques of gas laminar and turbulent pipe flow, Int. J. Heat Mass Transfer 111 (2017) 467–483.
[11] S.J. Kline, F.A. Mcclintock, Describing uncertainties in single-sample experiments, Mech. Eng. 75 (1953) 3–9.
[12] R.J. Moffat, Describing the uncertainties in experimental results, Exp. Therm. Fluid Sci. (1988) 3–17.
[13] B. Cheng, W.Q. Tao, Experimental study of R-152a film condensation on single horizontal smooth tube and enhanced tubes, J. Heat Transfer 116 (1994) 266–270.
[14] W.T. Ji, D.C. Zhang, N. Feng, J.F. Guo, M. Numata, G.N. Xi, W.Q. Tao, Nucleate pool boiling heat transfer of R134a and R134a-PVE lubricant mixtures on smooth and five enhanced tubes, J. Heat Transfer 132 (2010) 11502.
[15] F.P. Incropera, D.P. DeWitt, T.L. Bergman, A.S. Lavine, Fundamentals of Heat and Mass Transfer, John Wiley & Sons, 2011.
[16] J.H. Lienhard, A Heat Transfer Textbook, Courier Corporation, 2013.
[17] W. Nusselt, Die oberflachencondensation des wasserdampfes, VDI 60 (1916) 541–569.
[18] W.-T. Ji, G.-H. Chong, C.-Y. Zhao, H. Zhang, W.-Q. Tao, Condensation heat transfer of R134a, R1234ze(E) and R290 on horizontal plain and enhanced titanium tubes, Int. J. Refrig. 93 (2018) 259–268.
[19] W.-T. Ji, M. Numata, Y.-L. He, W.-Q. Tao, Nucleate pool boiling and filmwise condensation heat transfer of R134a on the same horizontal tubes, Int. J. Heat Mass Transfer 86 (2015) 744–754.
[20] W.-T. Ji, C.-Y. Zhao, D.-C. Zhang, Y.-L. He, W.-Q. Tao, Influence of condensate inundation on heat transfer of R134a condensing on three dimensional enhanced tubes and integral-fin tubes with high fin density, Appl. Therm. Eng. 38 (2012) 151–159.
[21] H. Blasius, Das Ahnlichkeitsgesetz bei Reibungsvorgangen in Flussigkeiten, Forsch. Arb. Ing.-Wes 131 (1913).
[22] W.-T. Ji, J.-F. Fan, C.-Y. Zhao, W.-Q. Tao, A revised performance evaluation method for energy saving effectiveness of heat transfer enhancement techniques, Int. J. Heat Mass Transfer 138 (2019) 1142–1153.
[23] Z. Zhang, Q. Li, T. Xu, X. Fang, X. Gao, Condensation heat transfer characteristics of zeotropic refrigerant mixture R407C on single, three-row petal-shaped finned tubes and helically baffled condenser, Appl. Therm. Eng. 39 (2012) 63–69.
[24] D. Jung, S. Chae, D. Bae, G. Yoo, Condensation heat transfer coefficients of binary HFC mixtures on low fin and Turbo-C tubes, Int. J. Refrig. 28 (2005) 212–217.
[25] D. Jung, C.-B. Kim, S.-M. Hwang, K.-K. Kim, Condensation heat transfer coefficients of R22, R407C, and R410A on a horizontal plain, low fin, and turbo-C tubes, Int. J. Refrig. 26 (2003) 485–491.
[26] M. Belghazi, A. Bontemps, C. Marvillet, Filmwise condensation of a pure fluid and a binary mixture in a bundle of enhanced surface tubes, Int. J. Therm. Sci. 41 (2002) 631–638.
[27] R.L. Webb, T.M. Rudy, M.A. Kedzierski, Prediction of the condensation coefficient on horizontal integral-fin tubes, J. Heat Transfer 107 (1985) 369–376.
[28] K.O. Beatty, Condensation of vapors on outside of finned tubes, Chem. Eng. Prog. 44 (1948) 55–70.
[29] J.-W. Ko, D.-S. Jeon, Y.-L. Kim, S.-C. Kim, Experimental study on film condensation heat transfer characteristics of R1234ze(E) and R1233zd(E) over horizontal plain tubes, J. Mech. Sci. Tech. 32 (2018) 527–534.
[30] S. Fukuda, C. Kondou, N. Takata, S. Koyama, Low GWP refrigerants R1234ze(E) and R1234ze(Z) for high temperature heat pumps, Int. J. Refrig. 40 (2014) 161–173.
[31] C. Kondou, F. Mishima, J. Liu, S. Koyama, Condensation and evaporation of R134a, R1234ze (E) and R1234ze (Z) flow in horizontal microfin tubes at higher temperature, 15th Int. Refrig. and Air Cond. Conf., Purdue, 2014, pp. 1446.